AUT Journal of Electrical Engineering
10.22060/EEJ.2025.23655.5628

Designing a robust method to improve virtual inertia control performance in islanded microgrid

Farhad Amiri[1]
[1]Department of Electrical Engineering, Tafresh University, Tafresh 39518-79611, Iran
f.amiri@tafreshu.ac.ir

Abstract: Power-electronic converters play a crucial role in the functioning of microgrids. However, these converters, characterized by their low inertia, present a significant challenge to maintaining a consistent frequency in islanded microgrids. To address this issue, an innovative concept known as virtual inertia control has emerged as a promising solution for enhancing frequency stability in islanded microgrids. The virtual inertia control system does not perform well against disturbances and uncertainty related to microgrid parameters. Therefore, to overcome these problems, it needs a suitable controller in its structure. In this paper, a linear quadratic regulator mode feedback controller based on deep learning is proposed to improve the performance of virtual inertia control in an islanded microgrid against disturbances and uncertainties in the system. The linear quadratic regulator controller uses measurements of system states and the integration of a deep network increases the accuracy and dynamic response of the feedback controller. This allows for fine-tuning of the control response, which exhibits significant robustness against uncertainty in system parameters and disturbances. To evaluate its effectiveness and compare it against alternative control approaches, comprehensive assessments have been conducted across multiple scenarios. The results indicate that the proposed method in the field of virtual inertia control surpasses previous approaches.

Keywords: Virtual inertia control; Linear quadratic regulator; Deep learning; Performance

1. Introduction

The frequency stability of an islanded microgrid is significantly influenced by the system's inertia [1-3]. Power-electronic converters, which inherently exhibit minimal inertia, are used to facilitate energy exchange between the microgrid and renewable energy sources such as WT and PV systems. This characteristic of minimal inertia poses a considerable challenge to the frequency stability of the microgrid [4]. To address these challenges, several control strategies have been rigorously studied to improve frequency regulation in isolated microgrid. Notably, these include: 1) VIC 2) PC 3) SC [5-7]. These methods aim to mitigate the adverse effects of low inertia and bolster the microgrid's frequency stability. Among these, VIC stands out as the most dynamic, actively responding to load changes within the microgrid. In contrast, the PC and SC strategies exhibit slower dynamic responses under such conditions. The microgrid's capacity to adapt to variations in load is intrinsically linked to the amount of kinetic energy stored in its rotating components [8]. The absorption and transmission of kinetic energy within a microgrid are fundamentally governed by its inertia. Following disturbances or other events, PC mechanisms typically require approximately 10 to 30 seconds to restore the frequency to a new stable state. In contrast, SC systems return the frequency to its nominal value within a significantly longer timescale, ranging from 30 seconds to 30 minutes after a deviation occurs. In this context, VIC emerges as a critical mechanism for ensuring frequency stability in an islanded microgrid [11]. As an integral component of virtual synchronous generators, VIC serves as the primary enabler for enhancing and sustaining frequency stability [12]. Beyond VIC, various energy storage technologies, such as batteries, hydrogen-based systems, and pumped hydro storage, can perform analogous functions in a microgrid. These systems can act as alternative VIC elements, effectively operating as virtual inertia sources by leveraging VIC technology to achieve performance comparable to Synchronous generator in conventional power systems [12-14]. However, the effectiveness

of VIC may be compromised under conditions involving significant disturbances or uncertainties in system parameters within an islanded microgrid [15].

In order to enhance the efficiency of VIC against these disruptions and unpredictabilities arising from system attributes, multiple control methods have been employed [16–42].

1-1-Literature review

In [16], the efficiency of VIC in islanded microgrids was found to be enhanced by implementing a fuzzy controller. Nevertheless, the utilization of a fuzzy controller faces limitations due to its demanding and complex design. A significant drawback of fuzzy controllers resides in their inefficiency when faced with disruptions occurring within the islanded microgrids, such as load disruptions or interruptions in renewable energy sources [17]. Researchers suggested a new approach, presented in [17], to address this problem. This approach involves using a technique with a variable droop coefficient that is suitable for microgrids operating in an islanded mode. This method contributed to some extent towards improving the VIC capabilities of microgrids while also providing increased flexibility for said grids that operate without connection to the main power supply. However, it is worth noting that this approach's effectiveness against disruptions within islanded microgrids is still not entirely satisfactory. In studies [18-20], a MPC approach has been employed to enhance the efficiency of VIC within microgrids. By leveraging an accurate microgrid model, the MPC controller can deliver satisfactory performance for VIC. However, a notable limitation of the MPC controller lies in its strong dependency on the availability of an exact microgrid model. The absence of such a model inevitably degrades the system's overall performance. Furthermore, under uncertain operating conditions, the effectiveness of MPC diminishes significantly. To address these challenges and improve the resilience of VIC in the face of uncertainties and disturbances, researchers have explored the implementation of an H∞ controller, as detailed in [21, 22]. This controller is designed to exhibit robustness against various disruptions encountered in microgrids and aims to minimize their adverse effects. Moreover, it demonstrates an enhanced ability to handle uncertainties in microgrid parameters, making it a promising solution for dynamic and unpredictable scenarios.

Despite its advantages, the H∞ controller is not without its limitations. Its performance, like that of the MPC controller, is heavily reliant on the availability of an accurate system model. Inaccuracies in the model can compromise its effectiveness. Additionally, the integration of the H∞ controller into an islanded microgrid presents significant challenges due to the complexity of its design and implementation. Overcoming these obstacles is critical for harnessing the full potential of this control strategy in practical microgrid applications. In [23], the paper discusses a study that aims to enhance the performance of VIC within the microgrid. The improvement is achieved through the adoption of an adaptive VIC, which incorporates a bang-bang control mechanism. One of the key shortcomings of this control system is its performance degradation in the presence of disruptions and generating sources. In [24], the coefficient diagram approach is implemented to control the microgrid in a distinct manner. This approach has its drawbacks as it involves complicated computations and does not provide adequate protection against fluctuations in the load. On another note, [25] introduces a neuro-fuzzy network into the structure of VIC used in the microgrid with aims to control frequency. However, one must consider that implementing this method faces computational complexity challenges when applied to VIC. In [26], an innovative technique called the RPWFNN was employed within the structure of VIC in order to regulate frequency and enhance stability in the islanded microgrid. Moreover, in [27] and [28], a novel and advanced dynamic controller has been utilized to improve the functionality of VIC in isolated microgrids with single or multiple areas. This approach demonstrates remarkable resistance against disturbances and uncertainties caused by

different microgrid factors. However, to achieve successful implementation, it is crucial to have a precise model of the microgrid and perform complex calculations associated with it. The traditional PID controller is highly regarded and widely used in the field of electrical engineering [29]. Its popularity stems from its simplicity, user-friendliness, rapid response time, and ability to maintain stability when controlling the frequency of the microgrid. In the context of islanded microgrids, various controllers have been employed to regulate frequency and enhance stability [29-36]. The controllers used in this study are PI controllers [29, 30], PID controllers [31], PID controllers implemented with the ZN method [32], PID controllers implemented with GA [33], PID controllers implemented with PSO [34], PID controllers implemented with BBO [35], and PID controllers implemented with QOH [36]. It is important to mention that the traditional FOPID controller provides two degrees of freedom, while the standard PID controller only has one degree of freedom–there are several advantages associated with its use: heightened precision, improved stability, and robust performance even in systems affected by disruptions and uncertainties in parameters [37]. The frequency regulation of the microgrid was effectively managed through the utilization of the FOPID controller, as detailed in [38, 39]. Furthermore, additional studies ([39], [40], [41], and [42]) demonstrated how the performance and stability of the islanded microgrid's frequency were enhanced through various optimization techniques applied to the parameters of the FOPID controller. Specifically, a neural network was used for parameter tuning in one study, while other studies employed optimization methods such as SWA [40], SCA [41], and HSA [42]. These advancements exemplify significant contributions towards improving frequency stability within the microgrid system.

1-2-Novelty and contributions

The LQR controller is a significant method in the field of linear control and finds widespread use in the control industry [43]. This method relies on the mathematical model of the control system and employs linear objective functions to optimize system control by utilizing appropriate weight matrices. The LQR controller offers several benefits in the control industry [43]:

- Optimization: The LQR controller is optimized by formulating the linear objective functions as quadratic functions. This involves solving an optimization problem to determine the optimal weights in the control system. The system designer can carefully adjust these weights to achieve a more optimal result in system control.
- Accurate control: By utilizing the LQR controller, precise control can be applied to the system. The LQR adjusts the control input changes based on the current state of the system and the weights determined by the control designer. This results in higher accuracy in tracking and controlling the system's status.
- Stability: The LQR controller ensures system stability. Through appropriate weighting in the objective function, the optimal parameters of the controller can be computed, thereby keeping the system in a stable state. System stability is a critical objective in control systems.
- Adaptation to disturbances: As the system state or inputs change, the LQR controller reacts quickly and automatically and tries to restore the system to the desired state. This feature can be useful in the face of unexpected disturbances and system changes.
- Compatibility with constraints: LQR controller easily adapts to system constraints. Constraints such as input constraint, output constraint, physical constraint and other constraints can be easily considered in the mathematical model of the system and LQR objective function. These constraints are considered as optimization constraints and the LQR controller keeps the input and output within the allowed range.

In general, due to the above advantages, the LQR controller can significantly improve the control of industrial systems [43-46]. However, to fully exploit this method, it is necessary to have an accurate system

model and suitable objective functions. Also, the design and precise adjustment of LQR controller weights and parameters is also important.

In [43], the design of an LQR controller is discussed, incorporating the PSO and Kalman filter. In [44], the design of an LQR controller for the boost converter is explored, aimed at energy conservation. The LQR controller is designed for fuel cells [45], while in [46], the LQR controller design is discussed to enhance energy management strategies in batteries and super-capacitors. Based on the findings from [43] to [46], although the LQR controller offers notable advantages such as optimization, control accuracy, and stability, it also exhibits certain limitations and drawbacks. The following are the key limitations of the LQR controller:

- Sensitivity to unfavorable model: LQR controller needs accurate system model for optimization. If the system model is not correctly determined or there are discrepancies with the actual model, the performance of the LQR controller may decrease and have unpredictable results.
- Sensitivity to parameter changes: LQR controller is highly sensitive to parameter changes. If the system parameters are changed (such as friction coefficient, etc.), the performance of the LQR controller may not be improved and the parameters need to be reset.
- Limitation in nonlinear optimal control: LQR controller is suitable for linear systems and its performance may decrease in nonlinear systems. If the system is not linear or there are nonlinear changes in the system, using the LQR controller may lead to inappropriate settings and undesirable performance.
- Lack of long-term vision: The LQR controller usually focuses on the short-term objective function and optimization in the present. This means that its performance may deteriorate over longer distances and in conditions of continuous change. For problems that require long-term control and complex routing, the LQR controller alone may not be sufficient.

To overcome these limitations and defects, a common solution is to use feedforward neural network (FFNN). By combining the LQR controller with FFNN, better performance can be achieved in control-ling complex and nonlinear systems. FFNN can have the following advantages [47-51]:

- Ability to interact with complex environments: FFNN have the capability to approximate and learn complex patterns in input data. This enables them to effectively interact with intricate and nonlinear systems, outperforming pure LQR controllers.
- Adaptability to changes: FFNN possess the ability to automatically adapt to changes in the system. Whether there are modifications in system parameters or alterations in system behavior, the neural network can adapt dynamically and maintain optimal performance.
- Long-term control ability: FFNN are capable of learning routes and determining long-term control strategies. They can make informed decisions and select the appropriate control strategy based on past observations and potential future states.
- Resistance to model errors: FFNN can approximate and learn system performance without relying on an exact system model. This allows them to maintain acceptable performance even in the presence of errors or discrepancies in the system model.

The contributions of the article include the following:

- A LQR mode feedback controller based on deep learning is introduced to improve the performance of VIC performance in islanded microgrid
- Improving the performance of islanded microgrids against disturbances
- Improving the performance of islanded microgrid against uncertainties

- Reduction of frequency deviations related to islanded microgrid against disturbances

In this paper, a linear quadratic regulator (LQR) mode feedback controller based on deep learning is proposed to improve the performance of VIC in an islanded microgrid against disturbances and uncertainties in the system. The LQR controller uses measurements of system states and the integration of a deep network increases the accuracy and dynamic response of the feedback controller. This allows for fine-tuning of the control response, which exhibits significant robustness against uncertainty in system parameters and disturbances. To evaluate its effectiveness and compare it against alternative control approaches, comprehensive assessments have been conducted across multiple scenarios. Amongst these techniques are VIC based on H-infinite controller, VIC based on MPC controller. The results indicate that the proposed method in the field of VIC surpasses previous approaches.

1-3-Organization and structure of the paper

The forthcoming content of the paper is divided into various segments: Section 2 delves into an exploration of the investigated microgrid. In Section 3, our attention turns towards sketching the proposed controller in order to accomplish a desired VIC within the framework of said islanded microgrid structure. Moving ahead, a presentation of simulation outcomes and subsequent discussions ensue in Section 4. Ultimately, concluding thoughts are offered in Section 5.

2. The investigated microgrid

In this part, we shall discuss the various components of the investigated islanded microgrid as well as delve into the dynamic model of said microgrid.

2.1. The various components of the investigated microgrid

The configuration of the studied microgrid is illustrated in Figure 1 [21, 22]. This microgrid comprises a thermal power plant with a generation capacity of 12 MW, a WT capable of producing up to 7 MW, a PV system with a maximum output of 9 MW, a load demand capacity of up to 15 MW, and an energy storage system with a storage capacity of 4 MW. These components collectively form the operational foundation of the islanded microgrid under consideration [21]. Within this framework, The VIC is employed. This compensator is integrated into the energy storage system and is instrumental in maintaining equilibrium between generation and consumption [22].

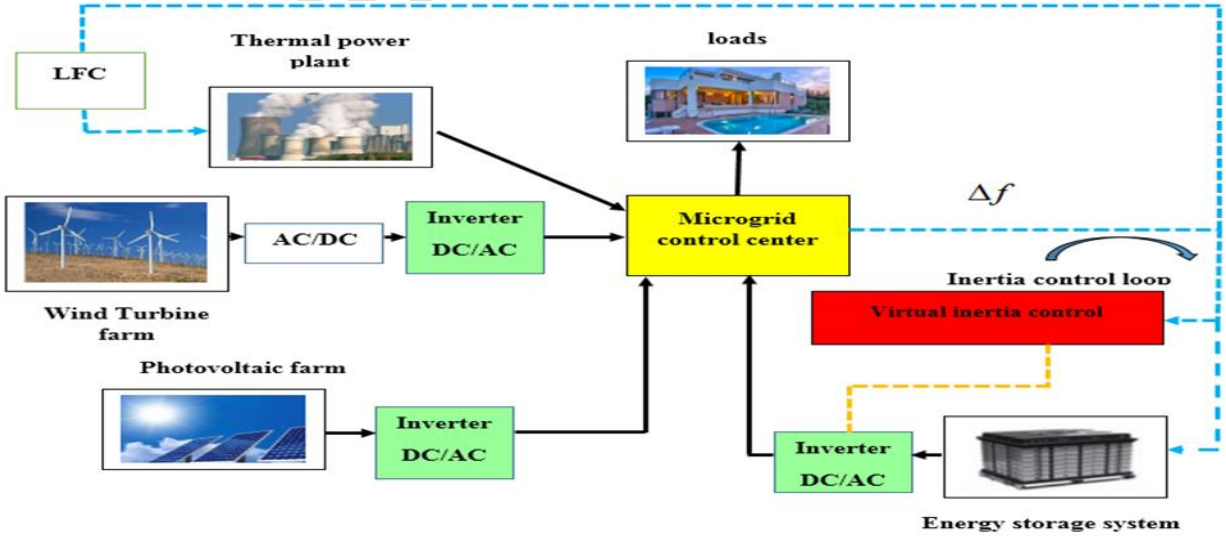

Figure 1. The structure of the studied microgrid [21, 22]

10.22060/EEJ.2025.23655.5628

2.2. The model used to analyze the behavior of the microgrid under study

The dynamic model related to the studied microgrid is studied through a dynamic model as shown in Figure 2. This model presents a detailed analysis of the microgrid [18–20]. The thermal power plant in this system includes a turbine with a limiter and a dead-band governor. The opening and closing speeds of the steam valve are represented by V_L and V_u respectively, accounting for their lowest and maximum values [18–20]. To ensure proper frequency regulation, a hierarchical control structure is implemented in the dynamic model of the microgrid. The structure of the controller is composed of three distinct control loops, namely the VIC loop, SC loop, and PC loop. In order to maintain stability, the main control loop incorporates a droop coefficient equal to *1/R* [18–20]. Furthermore, the SC loop contains both an integrator controller as well as a control error system with its corresponding gain K_I [21]. The microgrid being studied requires a common electrical system for frequency regulation that includes a transferring function of first-order. This function incorporates both a damping constant, *D*, and an inertia, *H*, to ensure proper balancing of the microgrid. WT systems and PV systems exemplify renewable energy sources, portrayed as first-order transfer functions with fortuitous inputs [21]. As depicted in Figure 2, the proposed controller (LQR based on deep learning) is employed within the VIC structure to augment the resilience of the self-sustained microgrid and uplift frequency steadiness. Table 1 presents the parameters associated with the microgrid [21, 22].

2.3. The equations of the state-space of the studied microgrid

The state-space equations of the studied microgrid are obtained by considering the VIC according to Equation (1) [22].

$$\begin{bmatrix} \dot{\Delta f} \\ \dot{\Delta P_m} \\ \dot{\Delta P_g} \\ \dot{\Delta P_{ACE}} \\ \dot{\Delta P_{inertia}} \\ \dot{\Delta P_W} \\ \dot{\Delta P_{PV}} \end{bmatrix} = \begin{bmatrix} \frac{-D}{2H} & \frac{1}{2H} & 0 & 0 & -\frac{1}{2H} & \frac{1}{2H} & \frac{1}{2H} \\ 0 & \frac{-1}{T_t} & \frac{1}{T_t} & 0 & 0 & 0 & 0 \\ \frac{-1}{RT_g} & 0 & \frac{-1}{T_g} & \frac{1}{T_g} & 0 & 0 & 0 \\ -\beta K_i & 0 & 0 & 0 & 0 & 0 & 0 \\ 0 & 0 & 0 & 0 & \frac{-1}{T_{ESS}} & 0 & 0 \\ 0 & 0 & 0 & 0 & 0 & -\frac{1}{T_{WT}} & 0 \\ 0 & 0 & 0 & 0 & 0 & 0 & \frac{-1}{T_{PV}} \end{bmatrix} \begin{bmatrix} \Delta f \\ \Delta P_m \\ \Delta P_g \\ \Delta P_{ACE} \\ \Delta P_{inertia} \\ \Delta P_W \\ \Delta P_{PV} \end{bmatrix} + \begin{bmatrix} 0 \\ 0 \\ 0 \\ 0 \\ \frac{K_{VI}}{T_{ESS}} \\ 0 \\ 0 \end{bmatrix} [u] + \begin{bmatrix} 0 & 0 & \frac{-1}{2H} \\ 0 & 0 & 0 \\ 0 & 0 & 0 \\ 0 & 0 & 0 \\ 0 & 0 & 0 \\ \frac{1}{T_{WT}} & 0 & 0 \\ 0 & \frac{1}{T_{PV}} & 0 \end{bmatrix} \begin{bmatrix} \Delta P_{wind} \\ \Delta P_{solar} \\ \Delta P_L \end{bmatrix}$$

$$y = [1 \quad 0 \quad 0 \quad 0 \quad 0 \quad 0 \quad 0] \begin{bmatrix} \Delta f \\ \Delta P_m \\ \Delta P_g \\ \Delta P_{ACE} \\ \Delta P_{inertia} \\ \Delta P_W \\ \Delta P_{PV} \end{bmatrix} \tag{1}$$

10.22060/EEJ.2025.23655.5628

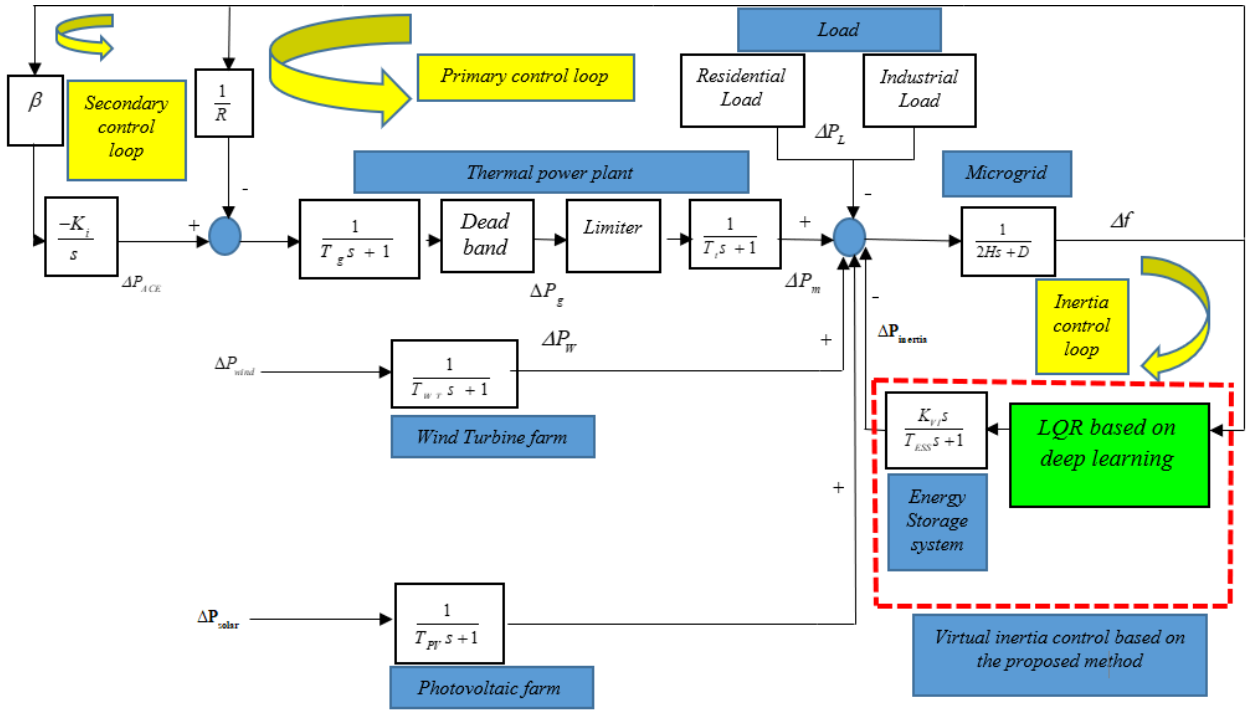

Figure 2. The dynamic model related to the studied microgrid

Table 1. The parameters associated with the microgrid [21, 22]

parameter	value	parameter	value
$T_{WT}(s)$	1.50	$B(pu.MW/Hz)$	1
$V_U\,(pu.MW)$	0.30	$T_{ESS}(s)$	10
$T_g(s)$	0.10	$D(pu.MW/Hz)$	0.0151
$T_t(s)$	0.40	$K_i(s)$	0.051
$T_{PV}(s)$	1.80	$R(Hz/pu.MW)$	2.42
$K_{VI}(s)$	0.50	$H(pu.MW/Hz)$	0.0833
$V_L\,(pu.MW)$	-0.30		

3. The proposed control method

3.1. The LQR controller

The LQR controller is an optimal control algorithm used to control continuous linear systems [43]. This optimal control method, using a quadratic cost function, tries to optimize the control input for the linear system to achieve specific goals such as error reduction, energy consumption reduction or system stability improvement [44]. In the LQR controller, the linear system is modeled with the differential relation according to Equation (2) [44-46].

$$\dot{x}(t) = Ax(t) + Bu(t) \qquad (2)$$

In equation (2), $x(t)$ is the state vector of the system, which includes different states of the system, $u(t)$ is the control input that is injected into the system. A is the system that shows the dependence between the states of the system. B is the control matrix that shows the dependence between the control input and the

system states. The objective of the LQR controller is to find an optimal control input that minimizes the quadratic cost function. The quadratic cost function is defined according to Equation (3) [44-46].

$$J(u)=\int_0^{\infty}\left[x^T(t)Qx(t)+u^T(t)Ru(t)\right]dt \quad (3)$$

In Equation (3), Q is the state cost matrix, which indicates the importance of each state of the system in the cost function. R is the control cost matrix, which indicates the importance of the control input in the cost function. To solve the optimization problem, Riccati's equations are used for the linear system. Riccati equations are defined according to Equation (4) [44-46].

$$Q-A^TP-PA+PBR^{-1}B^TP=0 \quad (4)$$

In Equation (4), P is the Riccati matrix to be solved. By solving the Riccati equations, the P matrix is obtained, and then the control input is calculated in the form of Equation (5) [44-46].

$$u(t)=-R^{-1}B^TPx(t) \quad (5)$$

When the P matrix is obtained, the system can be optimally controlled using this control input.

The LQR controller has features such as stability, optimality, and accuracy. In summary, the LQR controller is an optimal control method that calculates the optimal control input for the continuous linear system using the quadratic cost function. This controller has the ability to improve system performance, simple design, and stability. In addition to the mentioned advantages, the LQR controller has some limitations and defects. Among these defects, we can mention the sensitivity to the undesirable model, the sensitivity to the change of the parameters, and the limitation in the non-linear optimal control. To overcome these limitations and defects, a common solution is to use feedforward neural networks. By combining the LQR controller with FFNN, they achieve optimal performance of VIC in an islanded microgrid against disturbances and uncertainties in the system.

3.2. Feedforward neural network (FFNN)

FFNN is one of the types of neural networks used to solve the problems of sequence processing and temporal data [49]. These networks are able to preserve past states and use them in future times, which allows them to maintain long-term relationships and model temporal dependencies [45, 46]. In Figure 3, an example of a FFNN is presented [47]. It is an acyclic-directed graph, meaning there are no connections or feedback loops in the network [48]. It has an input layer, an output layer, and a hidden layer [48]. The first layer of a neural network is the input layer [48]. The input layer is used to prepare and enter data or features into the network [48]. The output layer is the layer that provides the results and predictions [48]. The activation function used in this layer is different for different problems. A FFNN applies a series of functions to the input. By having multiple hidden layers, complex functions can be computed with simpler functions one after the other. In the general case (FFNN), you can have several hidden layers. Each node in each layer represents a neuron, which can be considered a processing unit in the neural network [49, 50].

10.22060/EEJ.2025.23655.5628

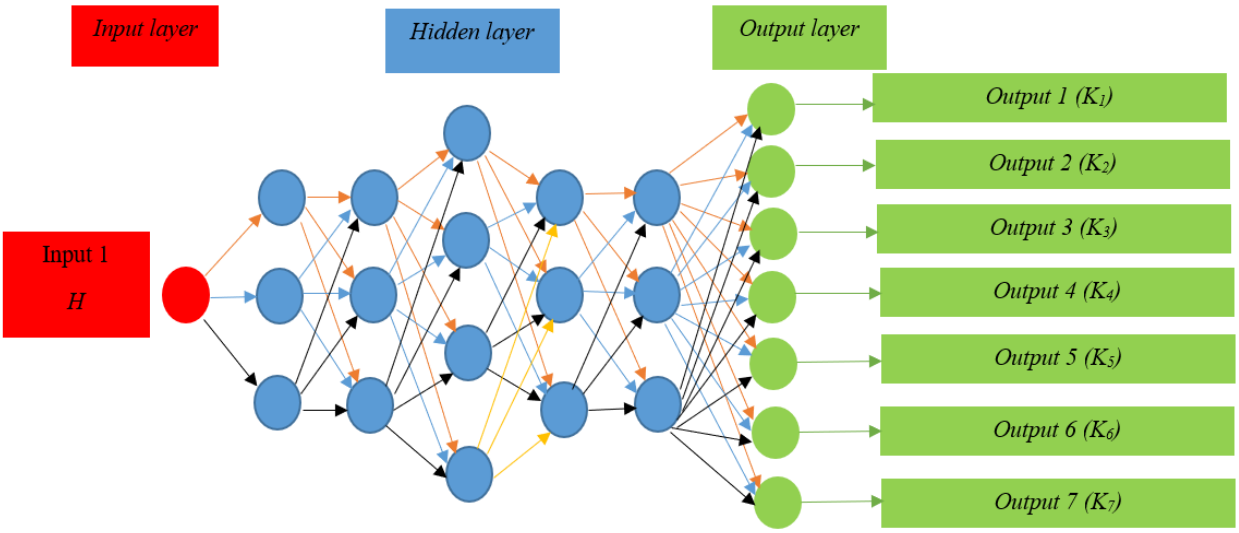

Figure 3. The FFNN

In Figure 4, the diagram of neural network neurons is shown, the neuron works in two steps: it calculates the weighted sum of the inputs and then applies an activation function to normalize this sum [47]. In this neuron, x_1 to x_n are equivalent to the inputs, W_1 to W_n are equivalent to the corresponding weights, and b represents the bias, and the f function is applied to the weighted sum of the inputs. Actuator functions can be linear or non-linear [48]. The activator function is used as a decision-making center in the output of a neuron. A neuron learns linear or non-linear decision boundaries based on the activation functions [49]. Also, this function normalizes the output of the neurons to prevent the output of the neuron from becoming too large after several layers. For each input of a neuron, there are corresponding weights. These are the parameters that the network must learn in the training phase [47-49].

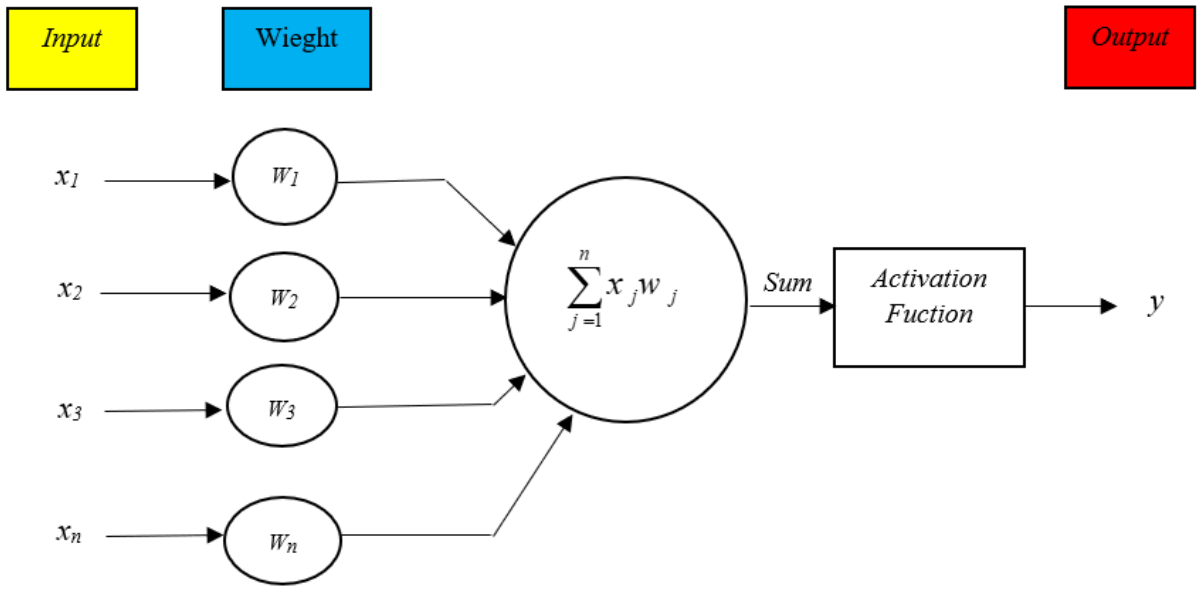

Figure 4. The diagram of neural network neurons

Training samples are fed into the network, and the resulting output is compared to the desired output. The error generated by this comparison is employed to iteratively adjust the weights of the neurons, gradually

minimizing the overall error. This weight adjustment process is accomplished through the utilization of the backpropagation algorithm.

3.3. The LQR controller design based on FFNN

The design of the LQR controller based on deep learning is proposed to improve the performance of VIC in an islanded microgrid against disturbances and uncertainties in the system. The LQR controller is one of the optimal control methods that designs the optimal controller based on the dynamic model of the studied microgrid and cost matrices. By using the FFNN, the cost function can be estimated and the parameters of the LQR controller can be optimized using this estimate. In other words, the FFNN can act as a cost function estimator and learn the optimal values for the LQR controller parameters. The design of an LQR controller based on deep learning is proposed to improve the performance of VIC and has advantages, including:

- Optimization: By utilizing an LQR controller based on a FFNN, the controller parameters can be optimally configured, resulting in improved performance compared to traditional methods.
- Flexibility: The neural network exhibits the capability to learn and adapt to changes in the studied microgrid parameters. Consequently, when there are alterations in the studied microgrid parameters, the neural network can be trained to automatically respond to these changes and maintain optimal control.

In Figure 5, an LQR controller structure-based FFNN structure is employed to improve the performance of VIC in an islanded microgrid against disturbances and uncertainties in the system. Since there is uncertainty in the *H* (inertia) parameter, it becomes necessary to update the gain (*K*) associated with the LQR controller to achieve the desired control objectives for the VIC. The FFNN is utilized to design the control gain, considering the uncertainties, in such a manner that the closed-loop system (consisting of the islanded microgrid with the proposed controller) remains stable over a wide range of parameter variations. Furthermore, it exhibits resilience to disturbances on the islanded microgrid while ensuring reference tracking capability.

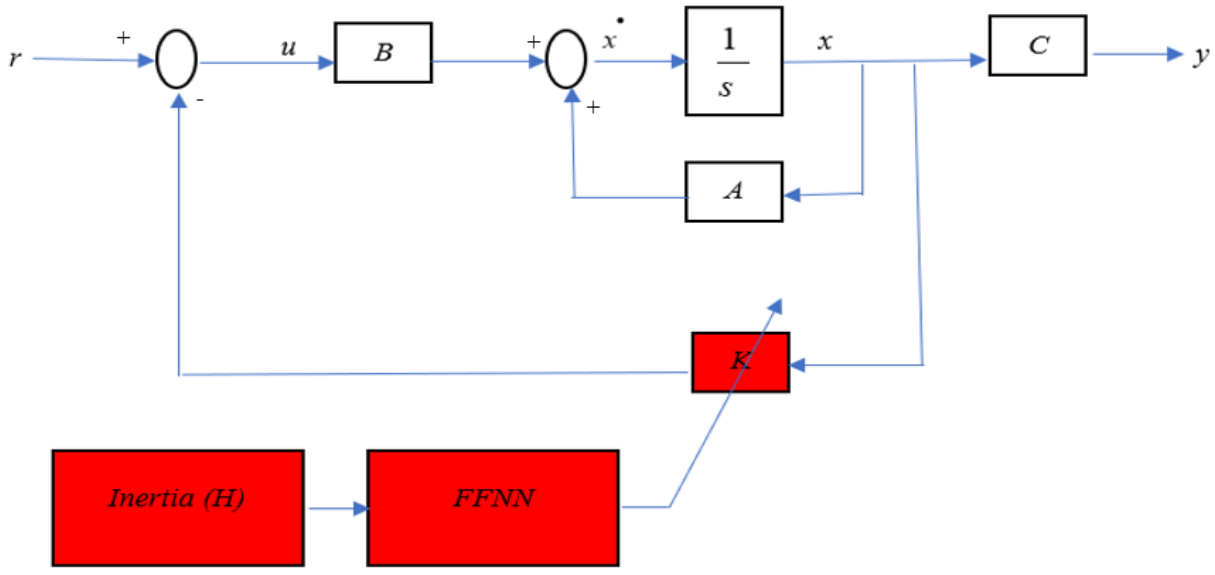

Figure 5. The LQR controller structure based FFNN structure is employed to improve the performance of VIC in an islanded microgrid against disturbances and uncertainties in the system.

4. Simulation Results and Discussion

10.22060/EEJ.2025.23655.5628

4.1. Designing the proposed controller in MATLAB

According to the Figure and Equations of the islanded microgrid stated in this paper, the proposed method has been designed in order to improve the performance of VIC against the uncertainty of system parameters and disturbances. To account for uncertainty in the *H* parameter, it was divided into 1000 points using MATLAB. For each of these points, the control gain (*K*) was determined. A FFNN was trained using the Levenberg-Marquardt algorithm to accomplish this. The FFNN consisted of 5 hidden layers, with the inertia (*H*) serving as the input and the LQR-related control gain (*K*) as the output. The training process was simulated using MATLAB software. Figure 6 depicts the training of the FFNN to determine the control gain (*K*), with a total of 398 iterations. The training duration was 1 second. Figure 7 shows the performance chart, indicating that the best performance was achieved in iteration 398, with a value of 6.01×10^(-5). The gradient and mu values were determined to be 0.00556 and 0.001, respectively. Figure 8 illustrates the error histogram. Furthermore, Figure 9 displays the regression for the training, validation, and test inputs, along with all the data. All the data points align along the y=x line, and the slope (R) of the line is equal to 1. This indicates that the neural network effectively mapped the relationship between *H* and *K*.

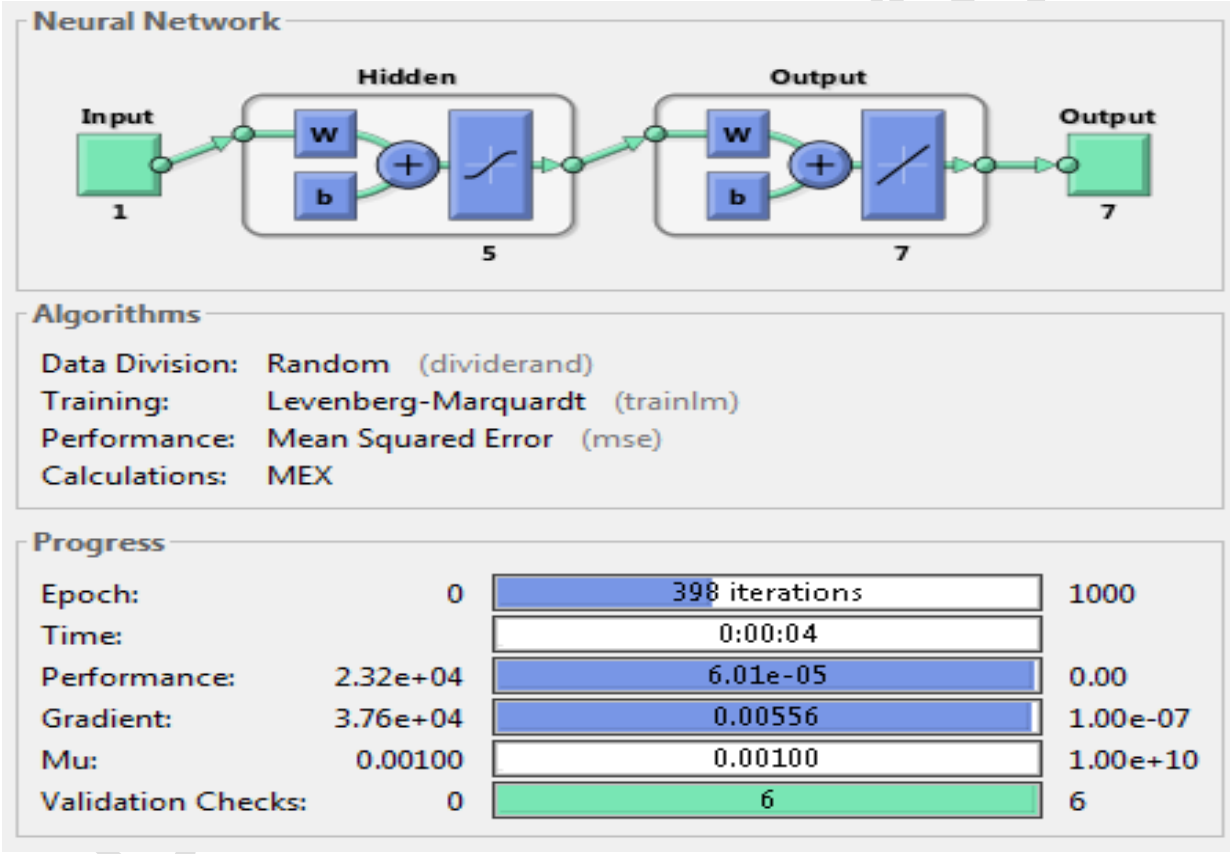

Figure 6. The training of the FFNN to determine the control gain (K)

10.22060/EEJ.2025.23655.5628

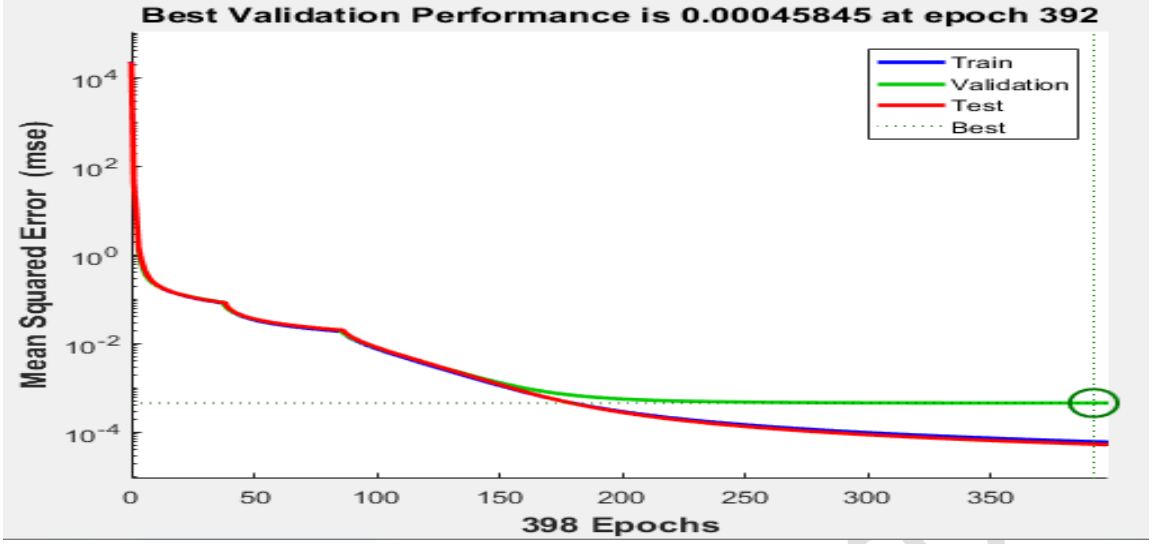

Figure 7. The performance chart

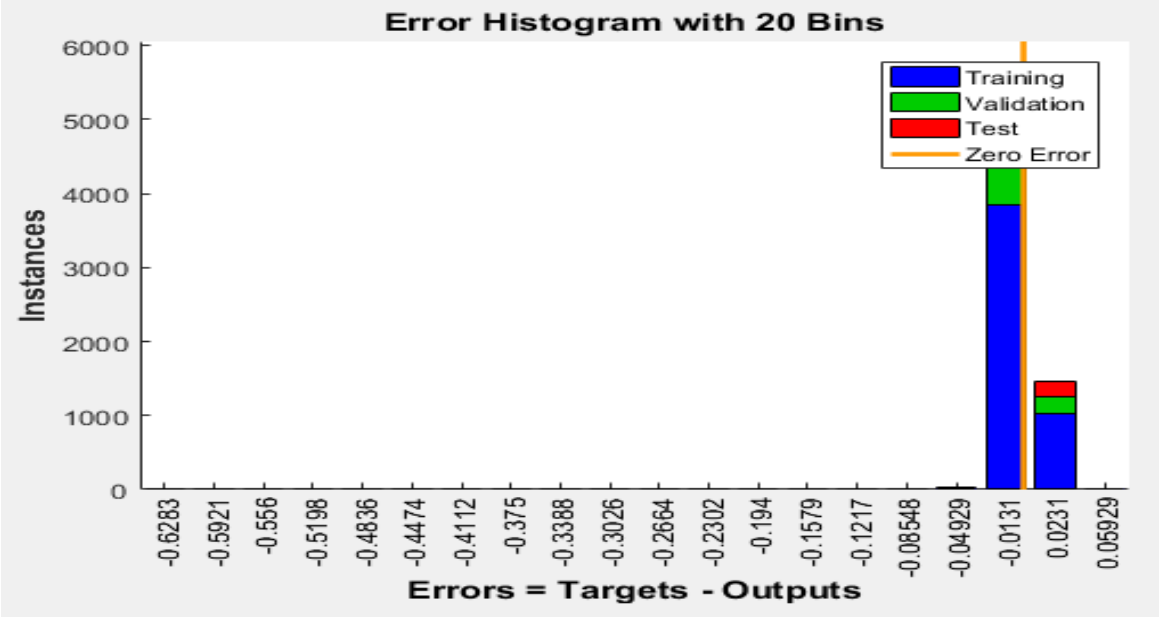

Figure 8. The error histogram diagram

10.22060/EEJ.2025.23655.5628

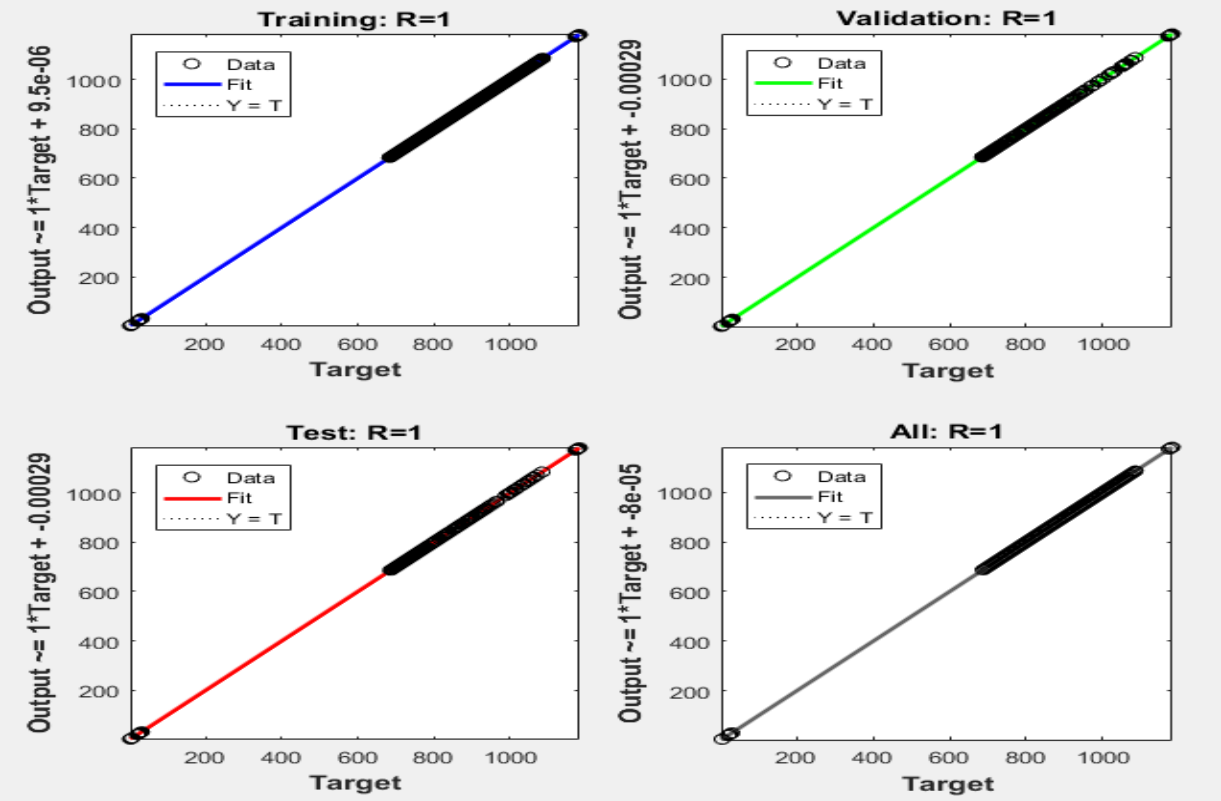

Figure 9. The regression for the training, validation, and test inputs, along with all the data

4.2. Scenario (1)

Within this particular scenario, a disruption of ΔP_L=0.1pu seamlessly integrates with the autonomous microgrid at t=1 seconds, as evident in Figure 10. The applied signal generated by the proposed controller for this microgrid can be observed in Figure 11. Additionally, Figures 12. a and 12. b exhibit Frequency response of the system employing various control strategies. To further analyze Scenario (1), referring to Table 2 presents results from different control methods utilized in this Scenario. Based on the data provided in Table 2, it is observed that the proposed method employing a VIC based on an LQR-FFNN controller yields an MFD of 0.0069 Hz and ST of 0.175 seconds. The MFD and ST using the VIC based on the H-infinite controller are 0.0391 Hz and 0.542 seconds, respectively. The MFD and ST using the VIC based on the MPC controller are 0.0763 Hz and 14.625 seconds, respectively. Concurring with the outcome of scenario (1), the proposed strategy has illustrated palatable execution compared to other utilized strategies in moderating the impacts of stack disturbances, altogether lessening recurrence deviations caused by stack disturbance. Also, the ST related to recurrence deviations caused by stack disruption has been quickened utilizing the proposed strategy.

10.22060/EEJ.2025.23655.5628

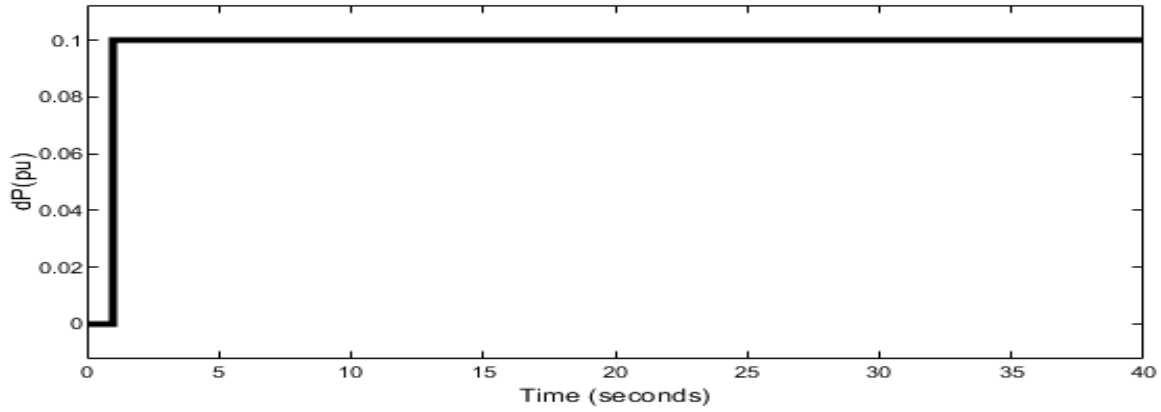

Figure 10. A disruption of the system

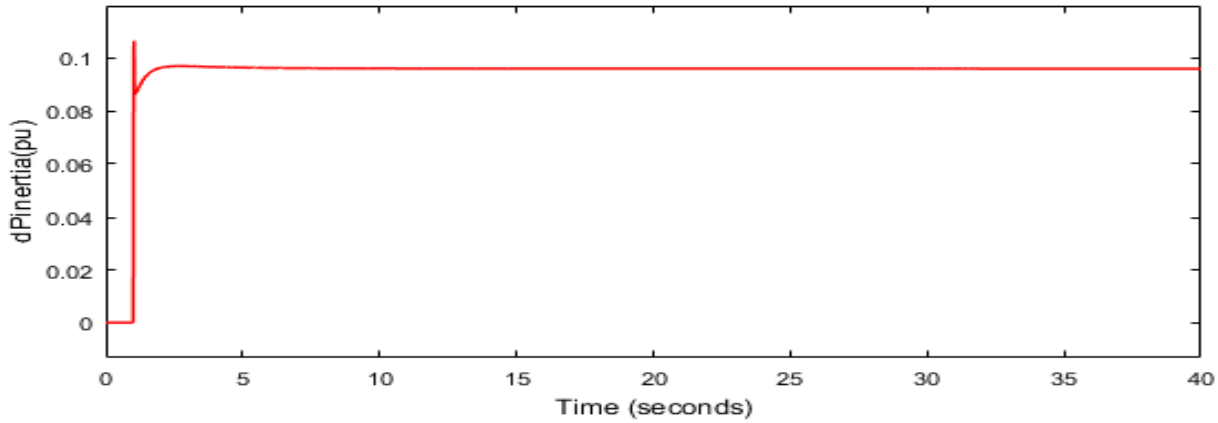

Figure 11. The signal generated by the proposed controller, Scenario (1)

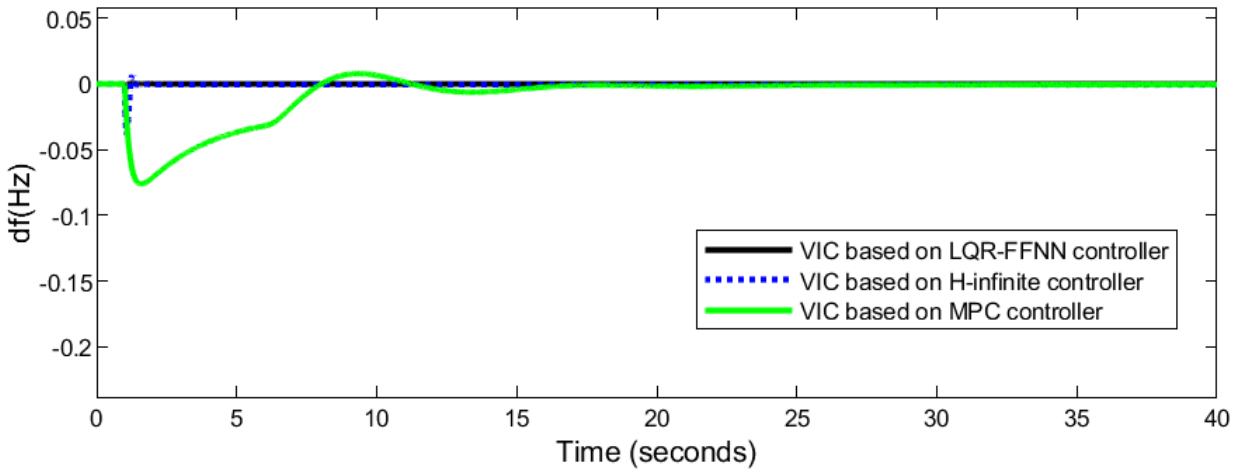

Figure 12.a. The Frequency response of the system, Scenario (1)

10.22060/EEJ.2025.23655.5628

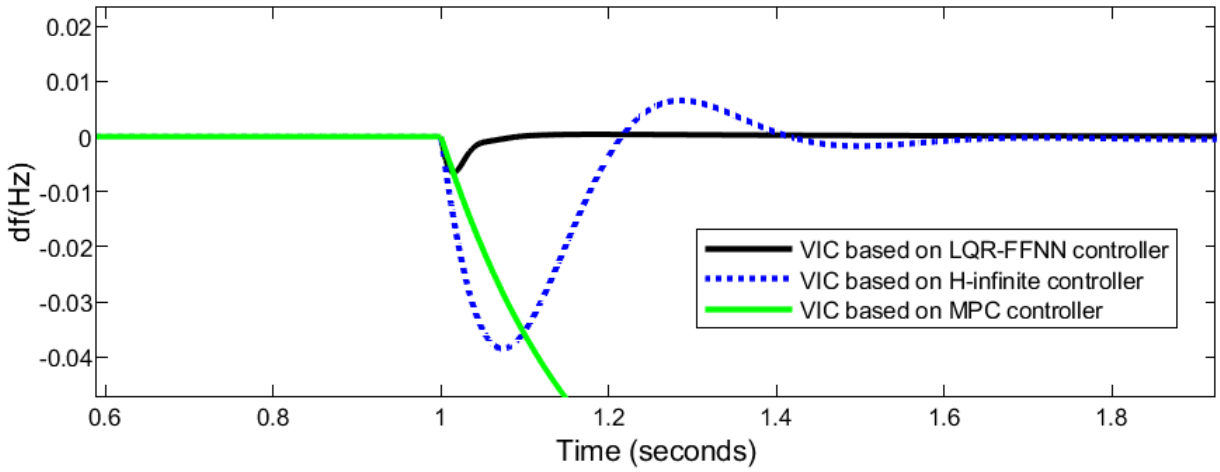

Figure 12.b. The Frequency response of the system, Scenario (1)

Table 2. The MFD and ST associated with frequency deviation utilizing various control strategies, Scenario (1)

Controller	MFD (Hz)	ST(sec)
VIC based on LQR-FFNN controller	0.0069	0.174
VIC based on H-infinite controller	0.0391	0.542
VIC based on MPC controller	0.0763	14.625

4.3. Scenario (2)

In this scenario, a stack disturbance has been presented to the system, taking under consideration the instability related with the parameters (*H=-50%*). The applied signal generated by the proposed controller for this microgrid can be observed in Figure 13. Figures 14. a and 14. b illustrate the Frequency response of the system with different control strategies, and Table 2 displays the results obtained from various control strategies in scenario (2). According to Table 3, the MFD and ST using the VIC based on the LQR-FFNN controller are 0.0083 Hz and 0.186 seconds, respectively. The MFD and ST using the VIC based on the H-infinite controller are 0.053 Hz and 0.77 seconds, respectively. The MFD and ST using the VIC based on the MPC controller are 0.10 Hz and 23.81 seconds, respectively. In light of the findings from scenario (2), the method put forth has demonstrated commendable effectiveness when juxtaposed with alternative methods employed in addressing disturbances and uncertainties tied to system parameters. It has proven particularly adept at diminishing frequency deviations induced by load disruptions, thereby mitigating their impact significantly. Furthermore, the proposed method has effectively expedited the ST associated with frequency deviations emanating from load disruptions and uncertainties stemming from system parameters.

10.22060/EEJ.2025.23655.5628

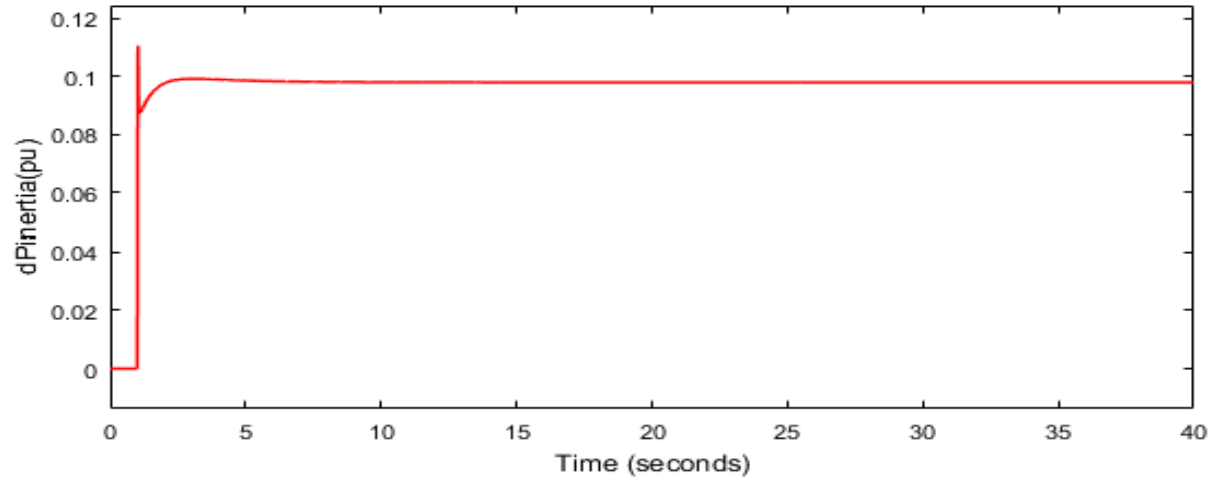

Figure 13. The signal generated by the proposed controller, Scenario (2)

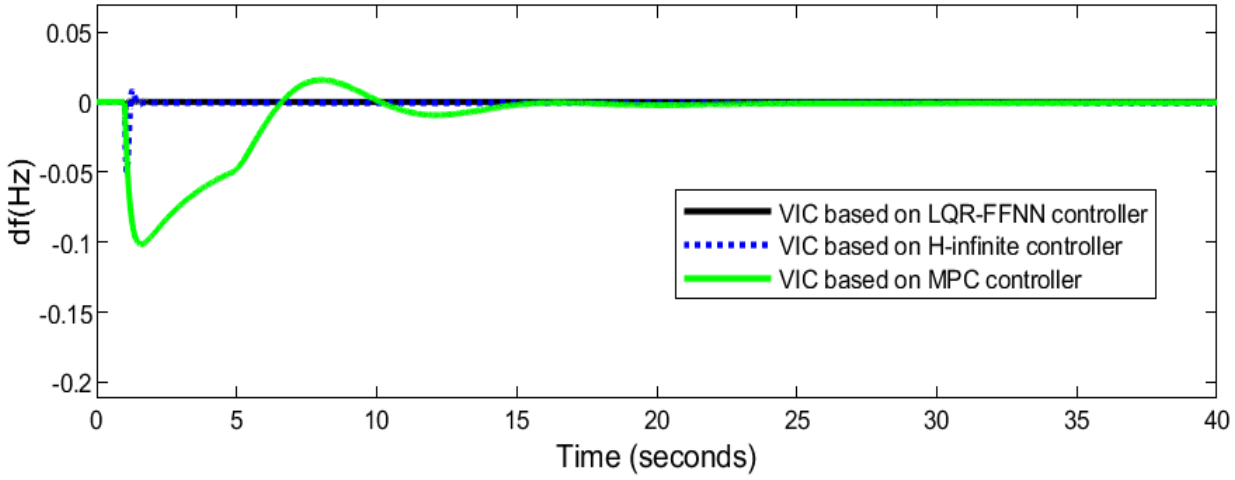

Figure 14.a. The Frequency response of the system, Scenario (2)

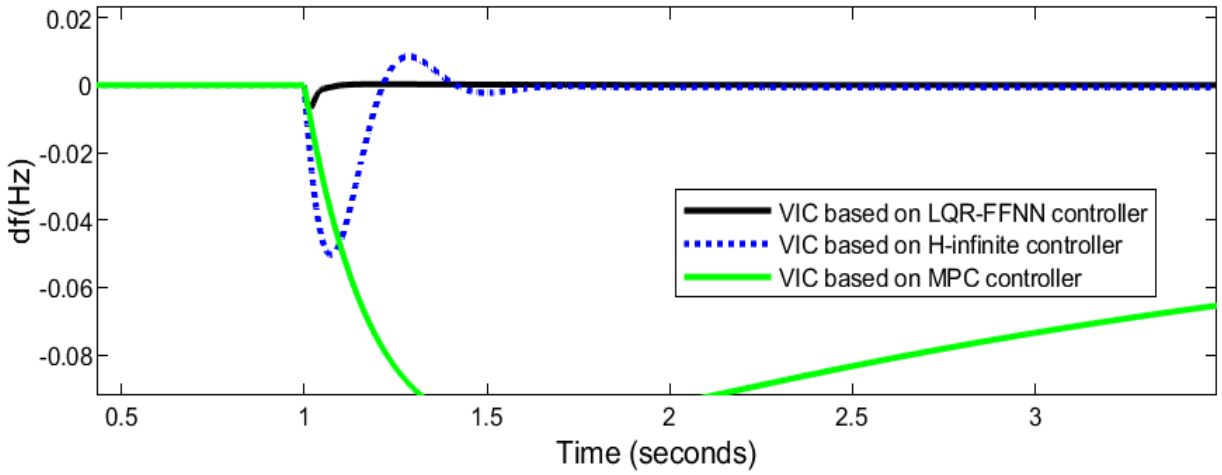

Figure 14.b. The Frequency response of the system, Scenario (2)

Table 3. The MFD and ST associated with frequency deviation using various control strategies, Scenario (2)

Controller	MFD (Hz)	ST(sec)
VIC based on LQR-FFNN controller	0.0083	0.186
VIC based on H-infinite controller	0.053	0.77
VIC based on MPC controller	0.10	23.81

4.4. Scenario (3)

Figure 15 presents a scenario where the system experiences both load disruptions and disruptions in WT. Moreover, a slight level of uncertainty (H=-5%) is taken into account for the microgrid parameters within this particular setting. The figure below portrays the signal applied by the proposed controller to operate the system (Figure 16). In Figure 17. a, 17. b, and 17. c, the Frequency response of the system using various control strategies is shown. Table 4 summarizes the outcomes of different control strategies applied for scenario (3). The MFD using VIC based on the LQR-FFNN controller is 0.0026 Hz. The MFD using VIC based on an H-infinite controller is 0.0053 Hz. The MFD using VIC based on an MPC controller is 0.04 Hz. Concurring with the comes about of scenario (3), the proposed strategy has performed well compared to other strategies in relieving the recurrence deviations caused by stack disturbances, renewable vitality source disturbances, and slight instability in framework parameters.

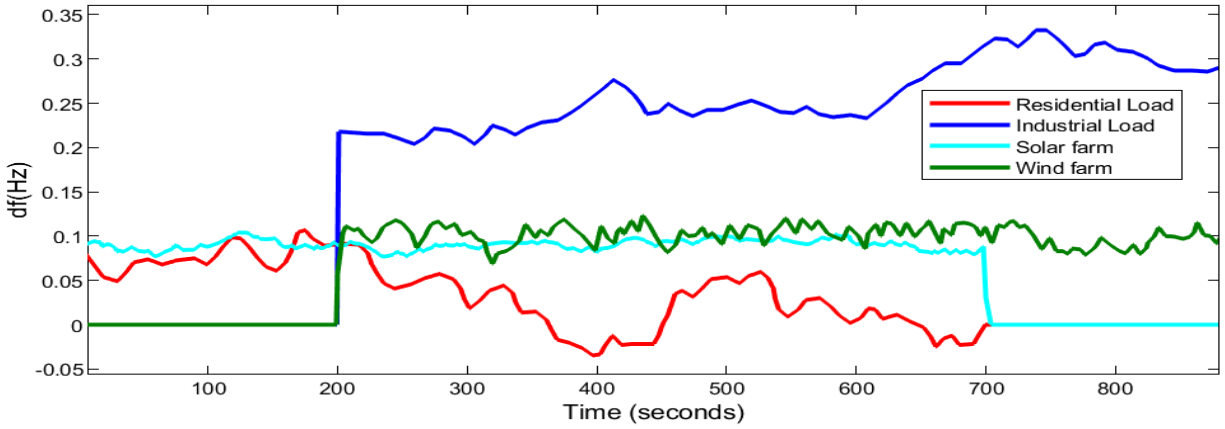

Figure 15. The disruptions in both load and renewable energy sources are imposed on the microgrid, Scenario (3)

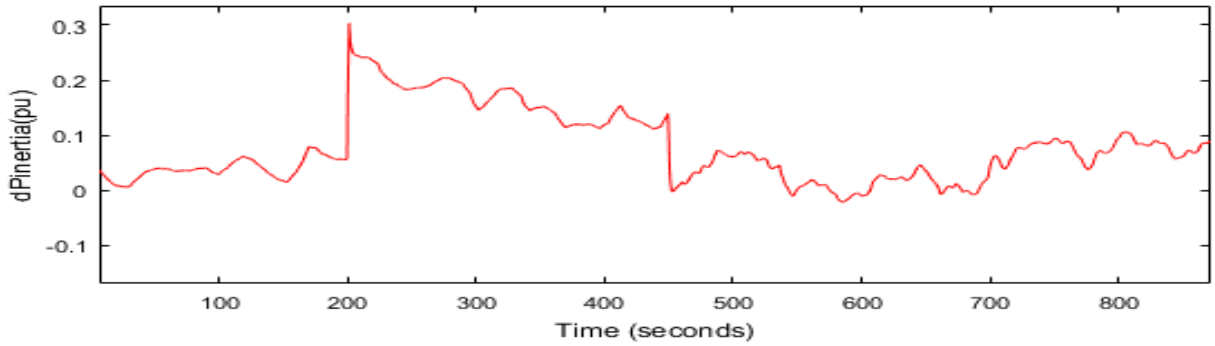

Figure 16. The signal generated by the proposed controller, Scenario (3)

10.22060/EEJ.2025.23655.5628

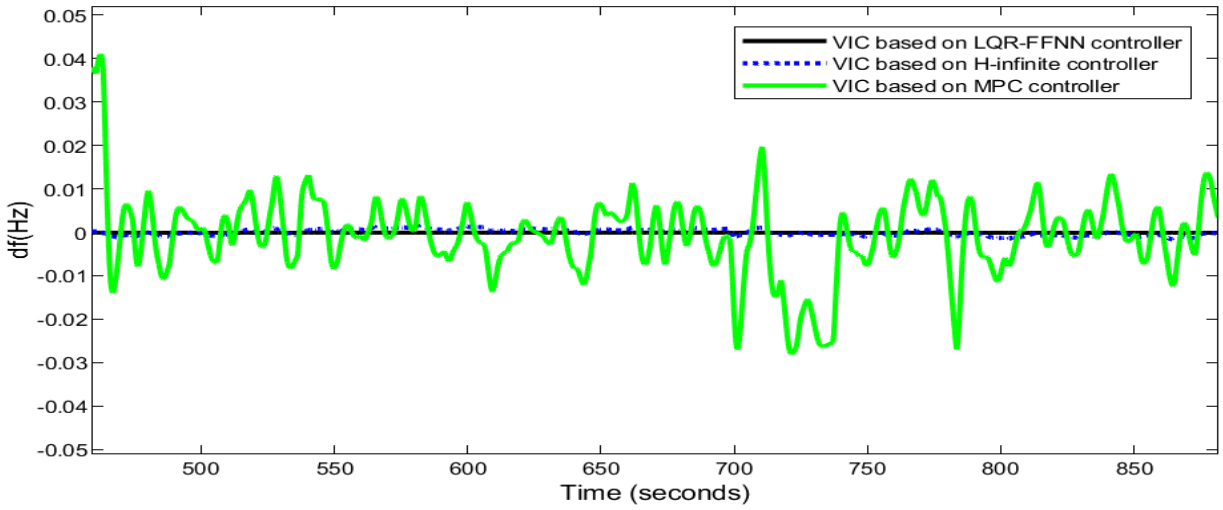

Figure 17.a. The FR of the system, Scenario (3)

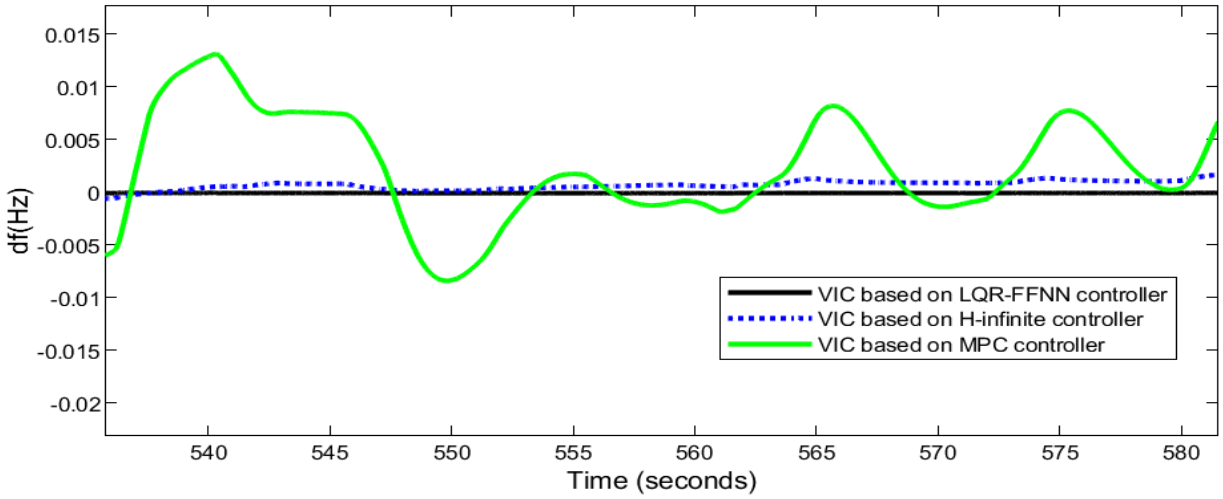

Figure 17.b. The FR of the system, Scenario (3)

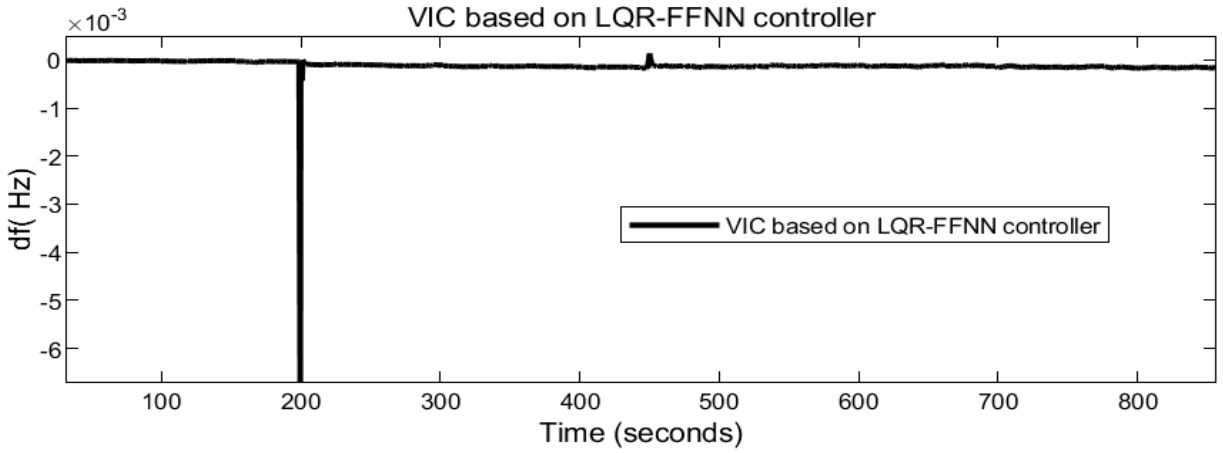

Figure 17.c. The FR of the system, Scenario (3)

Table 4. The MFD using various control strategies, Scenario (3)

Controller	MFD(Hz)
VIC based on LQR-FFNN controller	0.0026
VIC based on H-infinite controller	0.0053
VIC based on MPC controller	0.04

5. Conclusion

In this paper, a new and robust method was designed for the BESS to improve the performance of VIC against disruptions and uncertainties related to system parameters. An LQR mode feedback controller based on deep learning is proposed to improve the performance of VIC in an islanded microgrid against disturbances and uncertainties in the system. The LQR controller uses measurements of system states and the integration of a deep network increases the accuracy and dynamic response of the feedback controller. The proposed method (LQR based on deep learning) has the following advantages compared to other methods presented in the field of VIC related to the islanded microgrid.

• When compared to other methods, the studied system MFD is reduced by 81% in the event of load disturbances.

• When compared to other methods, the ST linked to the frequency variation of the studied system in the presence of load disturbances was reduced by 65%.

• Compared to other methods, the studied system MFD is reduced by 84% in the presence of load disturbances and uncertainty in system characteristics.

• Reduced the ST associated with the frequency deviation of the studied system by 74% when compared to alternative control approaches in the face of load interruptions and uncertainties in system characteristics.

• Compared to other methods, the studied system MFD is reduced by 95% in the face of load disturbances, WT interruptions, and modest uncertainty in system parameters.

• Reduction of the studied system MFD by 94% in the presence of load disruptions, WT disruptions, and substantial uncertainty in system parameters compared to alternative control approaches.

NOMENCLATURE:

WT	Wind Turbine	ΔP_L	Load Variations
PV	Photovoltaic	Δf	Frequency Variations
PC	Primary control	T_{ESS}	Time Constant of Energy Storage System
SC	Secondary control	ΔP_{wind}	Wind Turbine Power Variations
MPC	Model predictive control	ΔP_m	Thermal Power Plant Generated Power Variations
RPWFNN	Recyrrent probabilistic wavelet fuzzy neural network	ΔP_g	Governor Power Variations
ZN	Ziegler-Nichols	ΔP_{ACE}	Control Signal for Secondary Control

GA	Genetic Algorithm	T_{PV}	Time Constant of Photovoltaic System
PSO	Particle swarm optimization	T_{WT}	Time Constant of Wind Turbine
BBO	Biogeography-based optimization	T_t	Time Constant of Thermal Power Plant Turbine
QOH	Quasi-oppositional harmony	T_g	Time Constant of Governor
FOPID	Fractional order PID	ΔP_{solar}	Photovoltaic Power Variations
SWA	Salp swarm algorithm	K_{VI}	Gain for Virtual Inertia Control
SCA	Sine cosine algorithm		
HSA	Harmony search algorithm		
MFD	Maximum frequency deviation		
ST	Settling time		

REFERECE

1. S. Chen, J. Liu, Z. Cui, Z. Chen, H. Wang, & W. Xiao, A Deep Reinforcement Learning Approach for Microgrid Energy Transmission Dispatching, Appl. Sci, (14) (2024) 3682. https://doi.org/10.3390/app14093682

2. C.S. Makola, P.F. Le Roux, & J.A. Jordaan, Comparative Analysis of Lithium-Ion and Lead–Acid as Electrical Energy Storage Systems in a Grid-Tied Microgrid Application, Appl. Sci, (13) (2023) 3137. https://doi.org/10.3390/app13053137

3. F. Amiri & M.H. Moradi, Coordinated control of LFC and SMES in the power system using a new robust controller, Iranian Journal of Electrical and Electronic Engineering, 17(4) (2021) 1912-1912.

4. F. Amiri, M.H. Moradi, & M. Eskandari, Suppression of low-frequency oscillations in hybrid/multi microgrid systems with an improved model predictive controller, IET Renewable Power Generation (2024).

5. M. Tostado-Véliz, P. Arévalo, S. Kamel, R.A. El-Sehiemy, & T. Senjyu, Renewable-Based Microgrids: Design, Control and Optimization, Appl. Sci, (13) (2023), 8235. https://doi.org/10.3390/app13148235

6. F. Amiri, Virtual Inertia Control in a Two-Area microgrid Using Linear Matrix Inequality, Journal of Nonlinear Systems in Electrical Engineering 9(2) (2023) 85-115.

7. F. Amiri & M.H. Moradi, Design of a new control method for dynamic control of the two-area microgrid, Soft Computing 27(10) (2023) 6727-6747.

8. X. Zhang, Z. Zhu, Y. Fu, & W. Shen, Multi-objective virtual inertia control of renewable power generator for transient stability improvement in interconnected power system, International Journal of Electrical Power & Energy Systems, 2020 (117) (2020) 105641.

9. F. Amiri, M. Eskandari, & M.H. Moradi, Improved Load Frequency Control in Power Systems Hosting Wind Turbines by an Augmented Fractional Order PID Controller Optimized by the Powerful Owl Search Algorithm, Algorithms, (16) (2023), 539. https://doi.org/10.3390/a16120539

10. N.S Hasan, N Rosmin, N.M Nordin, S Abd Bakar, & A.H.M Aman, Dynamic response of hybrid energy storage based virtual inertial support in wind application, Journal of Energy Storage (53) (2022) 105181.

11. H. Abbou, S. Arif, & A. Delassi, Frequency Enhancement of Power System with High Renewable Energy Penetration Using Virtual Inertia Control Based ESS and SMES. In International Conference on Artificial Intelligence in Renewable Energetic Systems (2022), November, 602-613.

12. T. Kerdphol, F.S. Rahman, V. Phunpeng, M. Watanabe, & Y. Mitani, Demonstration of virtual inertia emulation using energy storage systems to support community-based high renewable energy penetration. 2018 IEEE Global Humanitarian Technology Conference (GHTC) (2018) 1-7.
13. V. Skiparev, J. Belikov, E. Petlenkov, & Y. Levron, Reinforcement learning based MIMO controller for virtual inertia control in isolated microgrids. 2022 IEEE PES Innovative Smart Grid Technologies Conference Europe (ISGT-Europe) (2022), 1-5.
14. W. Zeng, J. Xiong, & Z. Qi, DCNN-based virtual synchronous generator control to improve frequency stability of PV-ESS station. 2022 12th International Conference on CYBER Technology in Automation, Control, and Intelligent Systems (CYBER) (2022), 861-865.
15. B. Long, W. Zeng, J. Rodríguez, C. Garcia, J.M. Guerrero, & K.T. Chong, Stability Enhancement of Battery-Testing DC Microgrid: An ADRC-Based Virtual Inertia Control Approach. IEEE Transactions on Smart Grid 13(6) (2022) 4256-4268.
16. Y. Hu, W. Wei, Y. Peng, & J. Lei, Fuzzy virtual inertia control for virtual synchronous generator. *2016 35th Chinese Control Conference (CCC) (2016) 8523-8527.
17. C. Wang, J. Meng, Y. Wang, & H. Wang, Adaptive virtual inertia control for DC microgrid with variable droop coefficient. 2017 20th International Conference on Electrical Machines and Systems (ICEMS) (2017), 1-5.
18. T. Kerdphol, F.S. Rahman, Y. Mitani, K. Hongesombut, & S.K. Küfeoğlu, Virtual inertia control-based model predictive control for microgrid frequency stabilization considering high renewable energy integration, Sustainability, 9(5) (2017) 773.
19. A. Saleh, H.M. Hasanien, R.A. Turky, B. Turdybek, M.Alharbi, F. Jurado, & W.A. Omran, Optimal Model Predictive Control for Virtual Inertia Control of Autonomous Microgrids, Sustainability 15(6) (2023) 5009.
20. B. Long, W. Zeng , J. Rodríguez , J. M. Guerrero ,& K. T. Chong, Voltage regulation enhancement of DC-MG based on power accumulator battery test system: MPC-controlled virtual inertia approach . IEEE Transactions on Smart Grid 13(1) (2021) ,71-81.
21. T. Kerdphol, F.S. Rahman , Y. Mitani, M. Watanabe ,& S.K. Küfeoğlu, Robust virtual inertia control of an islanded microgrid considering high penetration of renewable energy, IEEE Access (6) (2017) 625-636.
22. F. Amiri & M.H. Moradi, Improving the MPC Performance of the Model in Order to Improve the Frequency Stability of the Two-Area Microgrid, International Journal of Industrial Electronics Control and Optimization2024 7(3) (2024) 175-185.doi:10 .22111/ieco .2024 .47435 .1517.
23. J. Li, B. Wen, & H. Wang, Adaptive virtual inertia control strategy of VSG for micro-grid based on improved bang-bang control strategy, IEEE Access (7) (2019) 39509-39514.
24. H. Ali, G. Magdy, B. Li, G. Shabib, A. A. Elbaset, D. Xu,& Y. Mitani, A new frequency control strategy in an islanded microgrid using virtual inertia control-based coefficient diagram method, IEEE Access2019 (7) (2019) 16979-16990.
25. A. Karimipouya, S. Karimi,& H. Abdi, Microgrid frequency control using the virtual inertia and ANFIS-based Controller, International of Industrial Electronics Control and Optimization 2(2) (2019) 145-154.
26. K.H. Tan, F.J. Lin, C.M. Shih, & C.N. Kuo, Intelligent Control of Microgrid with Virtual Inertia Using Recurrent Probabilistic Wavelet Fuzzy Neural Network, IEEE Transactions on Power Electronics (2019)
27. F. Amiri & M.H. Moradi, Designing a new robust control for virtual inertia control in the microgrid with regard to virtual damping, Journal of Electrical and Computer Engineering Innovations (JECEI) 8(1) (2020) 53-70.
28. M. H. Moradi & F. Amiri, Virtual inertia control in islanded microgrid by using robust model predictive control (RMPC) with considering the time delay, Soft Computing (25) (2021) 6653-6663.
29. R. Dhanalakshmi & S. Palaniswami, Load frequency control of wind diesel hydro hybrid power system using conventional PI controller, European Journal of Scientific Research (2011) 630-641.
30. D.I. Makrygiorgou & A.T. Alexandridis, Nonlinear modeling ,control and stability analysis of a hybrid ac/dc distributed generation system .In *2017 25th Mediterranean Conference on Control and Automation (MED) 2017 ,pp .768-773 .
31. B. Kumar & S. Bhongade,.Load disturbance rejection based PID controller for frequency regulation of a microgrid. In 2016 Biennial International Conference on Power and Energy Systems: Towards Sustainable Energy (PESTSE) 2016, pp. 1-6. IEEE.
32. F. Amiri & A. Hatami, Load Frequency Control Via Adaptive Fuzzy PID Controller In An Isolated Microgrid. In 32nd International Power System Conference, 2017, October.
33. D.C. Das, A.K. Roy, & N. Sinha, GA based frequency controller for solar thermal–diesel–wind hybrid energy generation/energy storage system, International Journal of Electrical Power & Energy Systems43(1) (2012) 262-279.

34. D.C. Das, A.K. Roy, & N. Sinha, PSO based frequency controller for wind-solar-diesel hybrid energy generation/energy storage system. In 2011 International Conference on Energy, Automation and Signal 2011, pp. 1-6. IEEE.

35. F. Amiri & M.H. Moradi, Improvement of Frequency Stability in the Power System Considering Wind Turbine and Time Delay, Journal of Renewable Energy and Environment 10(1) (2023) 9-18. doi: 10.30501/jree.2022.321859.1308
36. A. Kumar & G. Shankar, Quasi-oppositional harmony search algorithm based optimal dynamic load frequency control of a hybrid tidal–diesel power generation system, IET Generation, Transmission & Distribution 12(5) (2018), 1099-1108.
37. N. Divya, S. Manoharan, J. Arulvadivu, & P. Palpandian, An efficient tuning of fractional order PID controller for an industrial control process,Materials Today: Proceedings (57) (2022) 1654-1659.
38. S. Khosravi, M.T. Hamidi Beheshti, & H. Rastegar, Robust control of islanded microgrid frequency using fractional-order PID, Iranian Journal of Science and Technology, Transactions of Electrical Engineering (44) (2020), 1207-1220.
39. V. Skiparev, K. Nosrati, A. Tepljakov, E. Petlenkov, Y. Levron, J. Belikov,& J. M. Guerrero, Virtual Inertia Control of Isolated Microgrids Using an NN-Based VFOPID Controller, IEEE Transactions on Sustainable Energy (2023)
40. F. Babaei, Z. B. Lashkari, A. Safari, M. Farrokhifar, & J. Salehi, Salp swarm algorithm-based fractional-order PID controller for LFC systems in the presence of delayed EV aggregators, IET Electrical Systems in Transportation 10(3) (2020) 259-267.
41. F. Babaei & A. Safari, SCA based fractional-order PID controller considering delayed EV aggregators, Journal of Operation and Automation in Power Engineering 8(1) (2020) 75-85.
42. S. Asgari, A. A. Suratgar, & M. Kazemi, Feedforward fractional order PID load frequency control of microgrid using harmony search algorithm, Iranian Journal of Science and Technology, Transactions of Electrical Engineering 45(4) (2021) 1369-1381.
43. H. Maghfiroh, M. Nizam, M. Anwar, & A. Ma'Arif, Improved LQR control using PSO optimization and Kalman filter estimator, IEEE Access (10) (2022) 18330-18337.
44. D.O. Neacșu & A. Sirbu Design of a LQR-based boost converter controller for energy savings, IEEE Transactions on Industrial Electronics 67(7) (2019) 5379-5388.
45. N. Agrawal, S. Samanta,& S. Ghosh, Modified LQR technique for fuel-cell-integrated boost converter, IEEE Transactions on Industrial Electronics68(7) (2020) 5887-5896.
46. S. Ferahtia, A. Djeroui, T. Mesbahi, A. Houari, S. Zeghlache, H. Rezk, & T. Paul, Optimal adaptive gain LQR-based energy management strategy for battery–super capacitor hybrid power system, Energies 14(6) (2021) 1660.
47. P. Skondras, N. Zotos, D. Lagios, P. Zervas, K.C. Giotopoulos, & G. Tzimas, Deep Learning Approaches for Big Data-Driven Metadata Extraction in Online Job Postings, Information (14) (2023),585 . https://doi.org/10 .3390/info14110585 .
48. Y. Chen & S. Zhang, A Helium Speech Unscrambling Algorithm Based on Deep Learning, Information, (14) (2023) 189. https://doi.org/10 .3390/info14030189.
49. H. Ren, C. Xu, Y. Lyu, Z. Ma,& Y. Sun A thermodynamic-law-integrated deep learning method for high-dimensional sensor fault detection in diverse complex HVAC systems, Applied Energy (351) (2023) 121830 .
50. Y. Gao, S. Miyata, & Y. Akashi, How to improve the application potential of deep learning model in HVAC fault diagnosis: Based on pruning and interpretable deep learning method, Applied Energy (348) (2023) ,121591 .